New Potent Azomethine Prodrugs of the Histamine H3-Receptor Agonist (*R*)-α-Methylhistamine[1] Containing a Heteroarylphenyl Partial Structure[2] ☆

Michael Krause[a], Agnès Rouleau[b], Holger Stark[a], Peter Luger[c], Monique Garbarg[b], Jean-Charles Schwartz[b], and Walter Schunack[a]*

[a] Institut für Pharmazie, Freie Universität Berlin, Königin-Luise-Strasse 2 + 4, D-14195 Berlin, Germany

[b] Unité de Neurobiologie et Pharmacologie, Centre Paul Broca de l'INSERM, 2ter rue d'Alésia, F-75014 Paris, France

[c] Institut für Kristallographie, Freie Universität Berlin, Takustrasse 6, D-14195 Berlin, Germany

Key Words: *agonist; azomethine; histamine H3-receptor; prodrug*

Summary

The therapeutic value of histamine H3-receptor ligands is under current investigation. On the basis of recently described diaryl imine prodrugs of the histamine H3-receptor agonist (*R*)-α-methylhistamine (**1**) a series of new azomethine prodrugs containing five- and six-membered heterocycles were synthesized and tested for their *in vitro* hydrolysis rates and *in vivo* activity after oral application. It was found that electron-deficient six-membered heterocycles drastically destabilized the imine double bond so that these prodrugs decomposed unsuitably fast. On the contrary, prodrugs containing five-membered heterocycles appeared to be highly effective for the CNS delivery of **1**, and a remarkable correlation between chemical structure and pharmacokinetic profile was observed. Particularly (*R*)-4-fluoro-2-[[*N*-[1-(1*H*-imidazol-4-yl)-2-propyl]imino](1*H*-pyrrol-2-yl)methyl]phenol (**8c**), the 2-furanyl analogue **8d**, and its 3-furanyl isomer **8e** proved to be equipotent to the most potent of recently described halogenated diaryl imine prodrugs of **1**. However, in contrast to any other azomethine prodrug, **8c** exhibited an incomparably long lasting delivery of **1** in the CNS and can thus be regarded as a 'retard' prodrug. Assuming that a therapeutic indication of histamine H3-receptor agonists will soon be established, these highly potent heteroarylphenyl azomethine prodrugs, which already serve as valuable pharmacological tools, may also become potential drugs in clinical use.

Introduction

The suggestion of the existence of the histamine H3-receptor by Arrang *et al.* laid the foundation for the intensive study that has followed subsequently[1]. Meanwhile it is well established that histamine H3-receptors are not only presynaptic autoreceptors that control histamine synthesis in and release from histaminergic neurons[2, 3], but also modulate the release of a number of other neurotransmitters, e.g. acetylcholine[4], dopamine[5], noradrenaline[6], and serotonin[7]. Furthermore, it has been shown that histamine H3-receptors

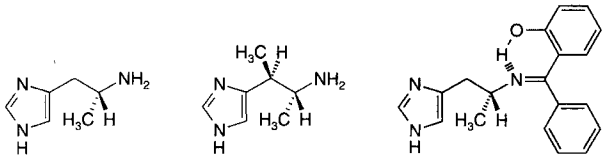

1 2 3

Figure 1: (*R*)-α-Methylhistamine (**1**), (α*R*, β*S*)-α,β-dimethylhistamine (**2**), and FUB 94 (**3**).

display their effects in distinct areas of the central nervous system (CNS)[8–10] as well as in several peripheral tissues like the digestive or the respiratory tract[11, 12]. The discovery that the chiral, side chain branched histamine derivative (*R*)-α-methylhistamine (**1**; Figure 1) is a potent and highly selective histamine H3-receptor agonist confirmed the existence of this receptor[13, 14]. It resulted in the frequent use of **1** as the standard histamine H3-receptor agonist in pharmacological studies, even though its more recently developed derivative (α*R*, β*S*)-α,β-dimethylhistamine (**2**; Figure 1) proved to be slightly more potent and selective[15]. Albeit **1** is very effective at histamine H3-receptors it appears to be poorly absorbed by the digestive tract and hardly delivered into the CNS[16] because of its strong basicity and polarity. In addition to these physico-chemical disadvantages **1** is rapidly inactivated by the important metabolizing enzyme histamine methyltransferase (HMT)[17, 18], and hence both its utilization as a pharmacological tool and its potential therapeutic application are limited. Thus, we recently prepared azomethine prodrugs in which **1** is bioreversibly linked to benzophenone derivatives in order to overcome those adverse pharmacokinetics[19–21]. Reduced basicity and enhanced lipophilicity as the result of this diaryl azomethine derivatisation lead to strikingly increased bioavailability and CNS penetration. Comparable GABAergic prodrugs like progabide[22] or fengabine[23] have been developed previously, but besides providing lipophilicity those prodrugs of **1** primarily prevented metabolization by HMT resulting in a further increase of tissue levels and prolonged activity[21]. The parent compound of these imine prodrugs, FUB 94 (**3**; Figure1), showed a 200-fold higher oral bioavailability compared to the single drug **1** but a limited brain penetration and

[1] Nomenclature of substituted histamine derivatives is based on the method of Black and Ganellin[31].

[2] Presented in part: XXIVth Annual Meeting of the European Histamine Research Society (EHRS), Moscow, Russia, May 20-25, 1995, and PCT Int. Appl[19].

  0365-6233/96/0404-0209 $5.00 + .25/0

is therefore at present under clinical investigation for indications linked to H_3-receptors in peripheral tissues[24].

In this study we report the introduction of heteroaromatic residues in an attempt to optimize the pharmacokinetic profile of those azomethine prodrugs. Halogenation of the phenolic residue was retained in most cases since it was previously found to be required for the CNS delivery of **1**[21]. The second phenyl ring of the pro-moiety was replaced by five- and six-membered heterocycles as the phenolic residue was discovered to be essential. It forms an intramolecular hydrogen bond which facilitates the formation and enhances the stability of the imine double bond. The three-dimensional structure of compound **8d** as derived from X-ray structure analysis is therefore presented in order to substantiate that crucial intramolecular hydrogen bond. Additionally, the resulting *in vitro* hydrolysis rates of these heteroarylphenyl azomethine prodrugs (**8**) were examined at different pH values as well as the biological activity *in vivo* after p.o. application to mice. It was thereby strengthened that the pharmacokinetic profile strikingly depended on the chemical structure, in particular on the heteroaromatic residue and its position of substitution.

Chemistry

Synthesis. The heteroaryl 2-hydroxyphenyl methanones **7** were prepared as described in Scheme 1. Firstly, the heteroarenecarboxylic acids **4** were converted to the corresponding acyl chlorides **5** by treatment with $SOCl_2$ and subsequently esterified with phenols in the presence of Et_3N[25]. The resulting esters **6** were rearranged in the presence of $AlCl_3$ according to Fries[26] giving the heteroaryl 2-hydroxyphenyl methanones **7**, although the yields were strongly suppressed from 70% for the oxygen containing heterocycles down to 10% for the nitrogen containing ones. The pro-moieties **7** and compound **1** were then refluxed in dry MeCN and repeatedly evaporated yielding the desired azomethines **8a–g** in a condensation reaction (substitution pattern of **8a–g** shown in Table 1). However, during chromatographic purification different chemical stability was observed comparing prodrugs of the six- (**8a**, **8b**) and five-membered heteroaryl type (**8c–g**). Compounds **8a** and **8b** were clearly less stable than **8c–g** towards minimal amounts of water contained in both silica gel and eluent, and therefore the use of dry eluents and silica gel was necessary to obtain pure azomethines. Finally, the structure of each compound was confirmed by IR (not shown), MS, ^{1}H NMR, UV/Vis, optical rotation, and elemental analysis (C, H, N).

X-ray Structure Analysis. It was previously demonstrated that the intramolecular hydrogen bond between the phenolic hydroxyl group and the imine nitrogen is of great importance for the synthesis of the azomethines, and furthermore for their use as oral prodrugs, because this hydrogen bond not only facilitates the formation of the imine double bond but also provides stability towards hydrolysis in aqueous solution[21]. As reference for the general conformation of **8a–g** the crystal structure of compound **8d** was determined by X-ray structure analysis (for details see Experimental Part).

The resulting molecular structure is illustrated in a stereo representation in Figure 2 in which the atomic numbering scheme is also given (graphic program SCHAKAL[27]). Only the relative structure of **8d** had to be derived with the configuration assigned in Figure 2, as the *R*-configuration of the α-carbon atom C(7) was known from the synthesis.

The existence of the intramolecular hydrogen bond in question was in fact confirmed as O(21)–H(21)···N(8) with distances O···N = 2.522 (4) Å and H···O = 1.51 (4) Å. This rather strong hydrogen bond induces the phenyl ring C(16)···C(21) to be almost coplanar with the imine double bond N(8)–C(9). In particular, the interplanar angle between the least-squares planes through C(16)···C(21) and the corresponding plane through N(8), C(9), C(7), C(10), C(16) is only 3.2 (1)°. Conversely, the furanyl plane C(10)···O(13) forms an angle of 116.6 (2)° with the phenyl ring plane.

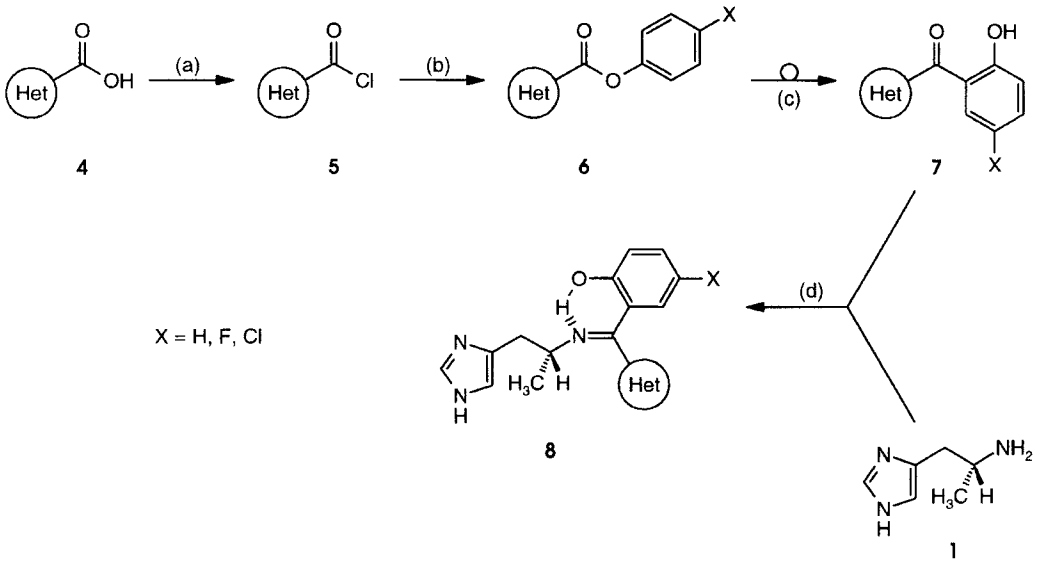

Scheme 1: General synthesis of heteroarylphenyl azomethine prodrugs of **1**[a].

[a] Reagents used: (a) $SOCl_2$, ambient temp. 18 h; (b) 4-X-PhOH, Et_3N/Et_2O, 1 h reflux; (c) $AlCl_3$, 150–180 °C for 20 min; (d) MeCN, 18 h reflux with repeated evaporation.

Table 1. Hydrolytic and pharmacokinetic data of heteroarylphenyl azomethine prodrugs of **1**.

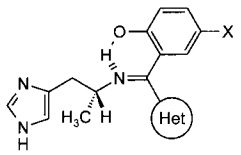

					Conversion rate (%)			AUC (**1**)		AUC (**8**)[a]	
					in vitro[b] after 2 h		*in vivo* after 6 h	plasma	CNS	plasma	CNS
No.	X	Het	Formula	M_r	pH 1	pH 7.4	plasma[c]	($ng \cdot h \cdot L^{-1}$)	($ng \cdot h \cdot g^{-1}$)	($ng \cdot h \cdot mL^{-1}$)	($ng \cdot h \cdot g^{-1}$)
8a	F	4-pyridinyl	$C_{18}H_{17}FN_4O \cdot 0.25H_2O$	328.9	100	100	–[d]	–[d]	–[d]	–[d]	–[d]
8b	H	4-pyrimidinyl	$C_{17}H_{17}N_5O \cdot C_2H_5OH$	353.4	100	–[d]	90	219	n.d.[e]	24	n.d.[e]
8c	F	2-pyrrolyl	$C_{17}H_{17}FN_4O \cdot 0.25H_2O$	316.9	24.5	52.1	20	247	97	1015	481
8d	F	2-furanyl	$C_{17}H_{16}FN_3O_2$	313.3	37.0	85.0	68	481	83	225	53
8e	F	3-furanyl	$C_{17}H_{16}FN_3O_2$	313.3	52.1	52.6	40	569	94	862	90
8f	F	2-thienyl	$C_{17}H_{16}FN_3OS$	329.4	42.1	43.0	38	726	56	1175	165
8g	F	3-thienyl	$C_{17}H_{16}FN_3OS$	329.4	67.4	69.2	27	649	24	1758	27

[a] AUC (**8**) is equivalent to **1** contained in the prodrug; [b] determined as ratio of free **1** to **1** contained in prodrug **8**; [c] AUC_{plasma} (**1**)/[AUC_{plasma} (**1**) + AUC_{plasma} (**8**)]; [d] – = not determined; [e] n.d. = not detectable.

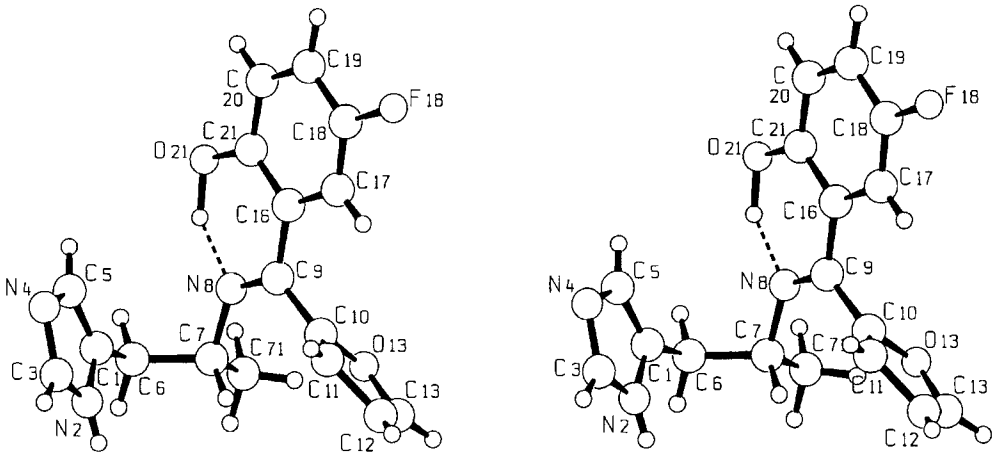

Figure 2: Stereo representation of the molecular structure of **8d** as derived from X-ray analysis.

The side chain conformation of the methylhistamine fragment can be described by the two torsion angles τ_1 = N(2)–C(1)–C(6)–C(7) and τ_2 = C(1)–C(6)–C(7)–N(8) which are determined as $\tau_1 = -80.4\ (4)°$ and $\tau_2 = -62.6\ (4)°$. Both τ_1 and τ_2 are of opposite sign compared to the previously determined structure of the (αR, βS)-α,β-dimethylhistamine dication (**2**), where these angles were around $\tau_1 = 82°$ and $\tau_2 = 64°$[15], and thus the side chain and the imidazole ring of **8d** are dissimilarly arranged.

Besides the intramolecular hydrogen bond an intermolecular hydrogen bond N(2)–H(2)···N(4)' is present in the crystal lattice of **8d** [N···N = 2.889 (4) Å, H···N = 2.09 (3) Å, symmetry operation for N(4)': $2 - x$, $-1/2 + y$, $1/2 - z$] generating infinite molecular chains along the screw axis in y-direction (crystal structures not shown).

Results and Discussion

***In Vitro* Results**. A previously developed sensitive and specific RIA allowed the determination of liberated amounts of **1** at various time intervals during the hydrolysis process. The hydrolysis rate of the prodrugs **8** was then calculated as the percent ratio of **1** determined in the sample to the corresponding value of complete hydrolysis (for details see Experimental Part)[21].

All heteroarylphenyl azomethine prodrugs of **1** prepared for this study were tested for their *in vitro* hydrolysis rates in both acidic and neutral medium after 2 h (Table 1). The striking difference between five- and six-membered heterocyclic substitution was thereby clearly indicated.

Immediate quantitative hydrolysis of the pyridinyl imine **8a** and the pyrimidinyl prodrug **8b** was observed following their dissolution in any aqueous medium. This is well consistent with the above mentioned lability noticed during chemical purification. Presumably the strong electron-withdrawing effect of those electron-deficient heterocycles accounts for this rapid decomposition, and therefore **8a** and **8b** were supposed to be unsuitably labile *in vivo*. On the basis of these results further investigations were focused on the more promising five-membered heterocycles.

Unlike the six-membered heterocycles the pyrrole-, furan-, and thiophene-containing prodrugs **8c–g** were significantly more stable in solution nevertheless displaying very heterogeneous hydrolysis profiles. Some prodrugs, namely the 2-pyrrolyl derivative **8c** and its oxo-analogue **8d**, exhibited a pH dependent hydrolysis both being more stable under acidic than neutral conditions. This is of particular interest if we compare **8d** and its isomer **8e** because the latter was not sensitive to pH variation. It was furthermore established that the exchange of furan oxygen by sulfur (**8f**, **8g**) abolished in fact the pH dependence of the conversion rates, but the 2-thienyl derivative **8f** proved to be clearly more stable than its position isomer **8g**. The most unique hydrolysis profile, however, was observed for the pyrrolyl azomethine **8c** that emerged to be distinct from any other prodrug of the azomethine type. Incubation at 95 °C in acidic medium did not markedly affect its conversion rate, so that complete hydrolysis, which is an essential step during determination, could not be achieved under standard conditions. In spite of this incomparable hydrolytic stability compound **8c** was after all completely hydrolyzed overnight at room temperature in neutral medium (see Experimental Part). On the basis of this observation one could probably expect an exceptional *in vivo* pharmacokinetic, too.

***In Vivo* Results**. The above-mentioned specific RIA for **1** also allowed the quantitative determination of drug and prodrug in both plasma and CNS. The *in vivo* level of **1** in plasma and cerebral cortex was determined directly like the *in vitro* determination, but conversely the corresponding prodrug level was calculated indirectly as the difference between the level of **1** measured in the sample before and after complete hydrolysis (for details see Experimental Part)[18, 21]. The observed plasma and CNS data are summarized as area under the curve values (AUC) in Table 1.

According to the above observations the pyrimidine derivative **8b** hydrolyzed immediately in the periphery after p.o. administration, perhaps for the greater part already in the digestive tract, and so almost no intact prodrug but only liberated **1** could be detected in the plasma. As a consequence the CNS delivery of **1** was not enhanced by **8b**. This observation was in accordance with the *in vitro* results proving the unsuitably low stability of azomethine prodrugs that contain six-membered heterocycles.

Unlike those unstable azomethines compounds **8cg** appeared to penetrate easily into the brain since all of them allowed to reach sufficient cerebral cortex levels of **1** after being orally administered. Nevertheless, striking differences were observed depending on the heteroaromatic residue and its position of substitution. Regarding the main objective of this development, the AUC of liberated **1** in the CNS, it is clearly indicated that the pyrrole derivative **8c** and the isomeric furanyl imines **8d** and **8e** showed the highest CNS levels of **1**. Although the 2-thienyl prodrug **8f** delivered lower CNS levels of **1** than the furanyl analogues **8d** and **8e** it was still more than twice as effective for the CNS delivery as its 3-thienyl isomer **8g**. However, the concentration-time curves determined for drug screening give a more detailed insight into the CNS pharmacokinetics (Figure 3). Apparently it points out the high C_{max} of **1** in CNS reached after the 2-substituted thiophene derivative **8f** (C_{max} = 48 ng/g), and even more after its 2-furanyl analogue **8d** attaining the particular value of 87 ng/g. Moreover, compounds **8d**, **8f**, and **8g** showed the same profile reaching their maximum values of liberated **1** after half an hour, and within 3 h the concentration value drops off to zero. As a matter of fact this pharmacokinetic profile was observed for every azomethine prodrug of **1** so far[21]. However, the pyrrolyl imine **8c** displayed an incomparably prolonged CNS pharmacokinetic of liberated **1** with a moderate C_{max} value of 21 ng/g, and even after 6 h an amount of 12 ng/g was detected. Compound **8c** can thus be regarded as a 'retard prodrug'. It has to be underlined that it was not possible to achieve prolonged pharmacokinetics to such an extent with formerly described benzophenone derived prodrugs[21].

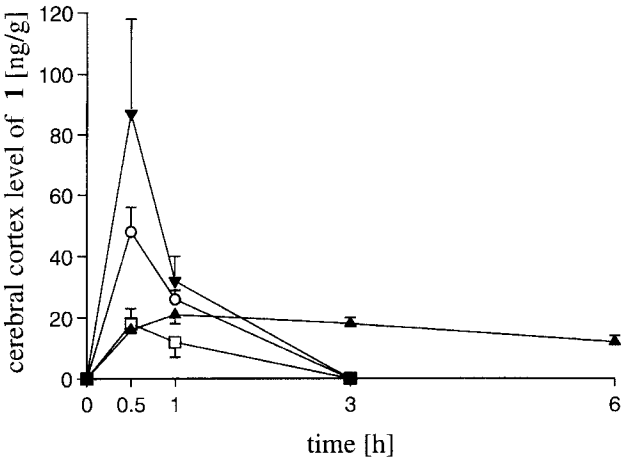

Figure 3: Cerebral cortex levels of **1** after p.o. administration of prodrugs **8c** (▲), **8d** (▼), **8f** (○), and **8g** (□) at a dose equivalent of 24 µmol of **1**/kg to mice.

Besides the absolute data the distribution of the active drug **1** is also of great interest from a therapeutic point of view, particularly when considering peripheral side actions. The ratio of liberated **1** in the CNS to the respective plasma value as given in Figure 4 emphasises the excellent CNS delivery of **1**, especially with **8c** and **8d**.

In conclusion, substitution with electron-donating heterocycles such as pyrrole, furan, or thiophene gives great CNS activity to imine prodrugs of **1**. In fact, these histamine H_3-receptor agonists are sufficiently stable, orally active and easily penetrating into the brain where histamine H_3-receptors are distributed in highest density. In addition, the pyrrolyl azomethine **8c** represents, to our knowledge, the first reported

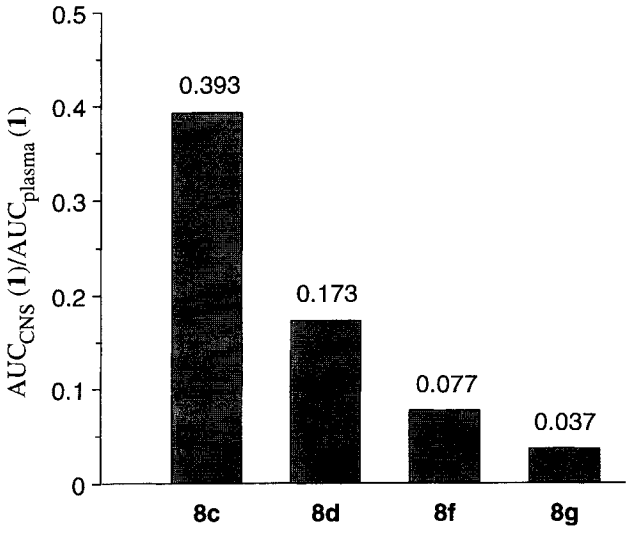

Figure 4: CNS ratio of **1** defined as AUC_{CNS} (**1**)/ AUC_{plasma} (**1**) after p.o. administration of **8c**, **8d**, **8f**, and **8g** at a dose equivalent of 24 μmol of **1**/kg to mice.

compound of the azomethine prodrug type, and particularly the first histamine H_3-receptor agonist to possess such prolonged *in vivo* pharmacokinetics.

Acknowledgement

We would like to thank Dr. J.-M. Lecomte (Bioprojet, Paris, France) for the generous gift of (*R*)-α-methylhistamine. We would also like to acknowledge the support by the Biomedical & Health Research Programme BIOMED I of the European Union (PL 921087) and by the Verband der Chemischen Industrie, Fonds der Chemischen Industrie (Frankfurt/Main, Germany).

Experimental Part

General Procedures. Melting points were determined on either an Electrothermal IA 9000 digital melting point or a Büchi 512 apparatus, and are uncorrected. All ^{1}H NMR spectra were recorded at 300 MHz on a Bruker AC 300 spectrometer. Chemical shifts are expressed in ppm downfield from internal Me_4Si as reference. ^{1}H NMR data are reported in order: multiplicity (*, exchangeable by D_2O; Fu, furanyl; Im, imidazolyl; Ph, phenyl; Py, pyridinyl; Pym, pyrimidinyl; Pyr, pyrrolyl; Th, thienyl), approximate coupling constants in hertz, and number of protons. Optical rotations were measured on a Perkin-Elmer 241 MC polarimeter. Furthermore, a Perkin-Elmer Lambda 15 UV/Vis spectrophotometer was used. Elemental analyses (C, H, N) were determined on either a Perkin-Elmer 240 B or C instrument, and were within ± 0.4% of the theoretical values unless otherwise indicated. TLC was performed on silica gel F_{254} plates (Merck). Column chromatography was carried out using silica gel 63–200 μm (Macherey, Nagel & Co.). Preparative, centrifugally accelerated, radial thin layer chromatography was performed using a Chromatotron 7924T (Harrison Research) and glass rotors with 4 mm layers of silica gel 60 PF_{254} containing gypsum (Merck).

Preparation of Heteroarene Carboxylic Acid Phenyl Esters 6. The carboxylic acid **4** (50 mmol) was stirred in excess $SOCl_2$ over night at room temperature yielding the corresponding acyl chloride **5** after evaporation *in vacuo*. Subsequently a solution of **5** in 20 mL Et_2O was added to a stirred solution of 4-fluorophenol (5.61 g, 50 mmol) and Et_3N (5.56 g, 55 mmol) in 150 mL Et_2O at a rate sufficient to maintain gentle reflux. The resulting suspension was then refluxed for 1 h, and the precipitated Et_3N·HCl was filtered off. The filtrate was washed ($NaHCO_3$, H_2O), dried ($MgSO_4$), and evaporated providing the crude ester **6** as a white solid, which was finally recrystallized from light petroleum (bp 50–70 °C).

*4-Pyridinecarboxylic Acid 4-Fluorophenyl Ester (**6a**)*

Yield 75%, mp 92 °C.– ^{1}H NMR (DMSO-d_6) δ = 8.90 (dd, ^3J = 4.5 Hz, J = 1.5 Hz, Py-2-H, Py-6-H), 8.01 (dd, ^3J = 4.5 Hz, J = 1.5 Hz, Py-3-H, Py-5-H), 7.36 (m, 4H, 4 Ph-H).– MS (70 eV); *m/z* (%) = 217 (22) [M^+], 106 (100) [$PyCO^+$]. Anal. ($C_{12}H_8FNO_2$).

*1H-Pyrrole-2-carboxylic Acid 4-Fluorophenyl Ester (**6c**)*

Yield 85%, mp 100 °C.– ^{1}H NMR (DMSO-d_6) δ = 12.21 (s*, 1H, NH), 7.28 (m, 4H, 4 Ph-H), 7.16 (s, 1H, Pyr-H), 7.03 (s, 1H, Pyr-H), 6.27 (d, J = 2.0 Hz, 1H, Pyr-H).– MS (70 eV); *m/z* (%) = 205 (10) [M^+], 94 (100) [$PyrCO^+$]. Anal. ($C_{11}H_8FNO_2$).

*2-Furancarboxylic Acid 4-Fluorophenyl Ester (**6d**)*

Yield 85%, mp 69.5 °C.– ^{1}H NMR (DMSO-d_6) δ = 8.12 (d, 1H, Fu-5-H), 7.59 (d, ^3J = 3.6 Hz, 1H, Fu-3-H), 7.33 (m, 4H, 4 Ph-H), 6.81 (dd, $^3J_{3\text{-H},4\text{-H}}$ = 3.6 Hz, $^3J_{4\text{-H},5\text{-H}}$ = 1.7 Hz, Fu-4-H).– MS (70 eV); *m/z* (%) = 206 (10) [M^+], 95 (100) [$FuCO^+$]. Anal. ($C_{11}H_7FO_3$).

*3-Furancarboxylic Acid 4-Fluorophenyl Ester (**6e**)*

Yield 99%, mp 48.5 °C.– ^{1}H NMR (DMSO-d_6) δ = 8.65 (s, 1H, Fu-2-H), 7.91 (m, 1H, Fu-5-H), 7.31 (m, 4H, 4 Ph-H), 6.95 (d, J = 1.7 Hz, 1H, Fu-4-H).– MS (70 eV); *m/z* (%) = 206 (10) [M^+], 95 (100) [$FuCO^+$]. Anal. ($C_{11}H_7FO_3$).

*2-Thiophenecarboxylic Acid 4-Fluorophenyl Ester (**6f**)*[23]

Yield 93%, mp 58 °C.– ^{1}H NMR (DMSO-d_6) δ = 8.11 (d, J = 5.0 Hz, 1H, Th-5-H), 8.03 (d, J = 3.8 Hz, 1H, Th-3-H), 7.32 (m, 5H, 4 Ph-H, Th-4-H).– MS (70 eV); *m/z* (%) = 222 (6) [M^+], 111 (100) [$ThCO^+$]. Anal. ($C_{11}H_7FO_2S$).

*3-Thiophenecarboxylic Acid 4-Fluorophenyl Ester (**6g**)*

Yield 77%, mp 53 °C.– ^{1}H NMR (DMSO-d_6) δ = 8.61 (dd, ^4J = 2.9 Hz, ^5J = 1.0 Hz, 1H, Th-2-H), 8.03 (dd, ^3J = 5.1 Hz, ^4J = 3.0 Hz, 1H, Th-5-H), 7.61 (d, ^3J = 5.1 Hz, 1H, Th-4-H), 7.32 (m, 4H, 4 Ph-H).– MS (70 eV); *m/z* (%) = 222 (8) [M^+], 111 (100) [$ThCO^+$]. Anal. ($C_{11}H_7FO_2S$).

Preparation of Heteroaryl-(2-hydroxyphenyl)methanones 7. To a stirred melt of **6** was added powdered $AlCl_3$ (1.2 equiv.). The mixture was heated for 20 min while the temperature was kept at 150–180 °C in order to reduce decomposition of the heteroaromatic residues, particularly the nitrogen containing ones. The obtained solid was pulverized and slowly added to a mixture of 2 N HCl and ice–water. The resulting suspension was extracted three times with Et_2O. The combined organic layers were then repeatedly washed ($NaHCO_3$, H_2O) and dried ($MgSO_4$). Evaporation to dryness yielded the crude ketone **7** as a yellow solid which was finally purified by column chromatography [eluent: CH_2Cl_2 (50%), light petroleum (50%)]. Ketone **7b** was commercially purchased.

*(5-Fluoro-2-hydroxyphenyl)-4-pyridinylmethanone (**7a**)*

Crystallized from Et_2O (16%), mp 109 °C.– UV/Vis (MeOH): λ_{max} = 348 nm.– ^{1}H NMR (DMSO-d_6) δ = 10.31 (s*, 1H, OH), 8.79 (d, J = 5.0 Hz, 2H, Py-2-H, Py-6-H), 7.59 (d, J = 5.8 Hz, 2H, Py-3-H, Py-5-H), 7.36 (m, 1H, Ph-4-H), 7.24 (dd, $^3J_{H,F}$ = 8.7 Hz, $^4J_{H,H}$ = 3.2 Hz, 1H, Ph-6-H), 6.99 (dd, $^3J_{H,H}$ = 9.0 Hz, $^4J_{H,F}$ = 4.5 Hz, 1H, Ph-3-H).– MS (70 eV); *m/z* (%) = 217 (48) [M^+], 106 (40) [M^+ – Py]. Anal. ($C_{12}H_8FNO_2$).

*(5-Fluoro-2-hydroxyphenyl)-1H-pyrrol-2-ylmethanone (**7c**)*

Crystallized from light petroleum (6%), mp 129 °C.– UV/Vis (MeOH): λ_{max} = 348 nm.– ^{1}H NMR (DMSO-d_6) δ = 12.07 (s*, 1H, NH), 10.25 (s*, 1H, OH), 7.25 (m, 3H, Ph-4-H, Ph-6-H, Pyr-H), 6.94 (dd, $^3J_{H,H}$ = 8.9 Hz,

$^4J_{H,F}$ = 4.5 Hz, 1H, Ph-3-H), 6.71 (s, 1H, Pyr-H), 6.24 (m, 1H, Pyr-H). MS (70 eV); *m/z* (%) = 205 (17) [M^+], 94 (100) [$PyrCO^+$]. Anal. ($C_{11}H_8FNO_2$).

(5-Fluoro-2-hydroxyphenyl)-2-furanylmethanone (**7d**)

Crystallized from light petroleum (70%), mp 74 °C.– UV/Vis (MeOH): λ_{max} = 354 nm.– ^{1}H NMR (DMSO-d_6) δ = 10.27 (s*, 1H, OH), 8.09 (s, 1H, Fu-5-H), 7.30 (m, 3H, Ph-4-H, Ph-6-H, Fu-3-H), 6.97 (dd, $^3J_{H,H}$ = 8.9 Hz, $^4J_{H,F}$ = 4.5 Hz, 1H, Ph-3-H), 6.75 (dd, $^3J_{3\text{-}H,4\text{-}H}$ = 3.5 Hz, $^3J_{4\text{-}H,5\text{-}H}$ = 1.6 Hz, 1H, Fu-4-H).– MS (70 eV); *m/z* (%) = 206 (63) [M^+], 138 (100) [M^+ – FuH]. Anal. ($C_{11}H_7FO_3$).

(5-Fluoro-2-hydroxyphenyl)-3-furanylmethanone (**7e**)

Crystallized from EtOAc/light petroleum (69%), mp 91–92 °C.– UV/Vis (MeOH): λ_{max} = 344 nm.– ^{1}H NMR (DMSO-d_6) δ = 10.38 (s*, 1H, OH), 8.33 (s, 1H, Fu-2-H), 7.86 (m, 1H, Fu-5-H), 7.31 (m, 2H, Ph-4-H, Ph-6-H), 6.98 (m, 1H, Ph-3-H), 6.87 (d, *J* = 1.5 Hz, Fur-4-H).– MS (70 eV); *m/z* (%) = 206 (100) [M^+], 189 (40) [M^+ – OH]. Anal. ($C_{11}H_7FO_3$).

(5-Fluoro-2-hydroxyphenyl)-2-thienylmethanone (**7f**)[23]

Crystallized from light petroleum (35%), mp 46–48 °C.– UV/Vis (MeOH): λ_{max} = 350 nm.– ^{1}H NMR (DMSO-d_6) δ = 10.04 (s*, 1H, OH), 8.09 (dd, ^3J = 4.9 Hz, ^4J = 1.1 Hz, 1H, Th-5-H), 7.56 (dd, ^3J = 3.8 Hz, ^4J = 1.1 Hz, 1H, Th-3-H), 7.24 (m, 3H, Ph-4-H, Ph-6-H, Th-4-H), 6.96 (m, 1H, Ph-3-H).– MS (70 eV); *m/z* (%) = 222 (44) [M^+], 189 (12) [M^+ – SH]. Anal. ($C_{11}H_7FO_2S$).

(5-Fluoro-2-hydroxyphenyl)-3-thienylmethanone (**7g**)

Crystallized from light petroleum (38%), mp 69 °C.– UV/Vis (MeOH): λ_{max} = 344 nm.– ^{1}H NMR (DMSO-d_6) δ = 10.16 (s*, 1H, OH), 8.16 (dd, $^4J_{2H,5H}$ = 2.8 Hz, $^5J_{2H,4H}$ = 1.1 Hz, 1H, Th-2-H), 7.65 (dd, ^3J = 5.1 Hz, ^4J = 2.8 Hz, 1H, Th-5-H), 7.46 (dd, ^3J = 5.1 Hz, ^4J = 1.1 Hz, 1H, Th-4-H), 7.25 (m, 2H, Ph-4-H, Ph-6-H), 6.96 (dd, $^3J_{H,H}$ = 8.9 Hz, $^4J_{H,F}$ = 4.5 Hz, 1H, Ph-3-H).– MS (70 eV); *m/z* (%) = 222 (56) [M^+], 189 (100) [M^+ – SH]. Anal. ($C_{11}H_7FO_2S$).

Preparation of Azomethines 8a–g. The final azeotropic azomethine condensation of **1** and **7** was attained under reflux in dry MeCN as recently published[21]. The reaction mixture was repeatedly evaporated at several time intervals to shift the equilibrium quantitatively to the product (TLC control). Finally the raw imine **8** was purified by preparative rotatory chromatography [eluent: CH_2Cl_2 (95–90%), MeOH (5–10%)].

(R)-(–)-4-Fluoro-2-[[N-[1-(1H-imidazol-4-yl)-2-propyl]imino]-(4-pyridinyl)methyl]phenol (**8a**)

Crystallized from EtOAc/C_6H_{12} (74%), mp 138–139 °C, $[\alpha]^{20}_D$ = *–209.3* (c = 0.01 in MeOH).– UV/Vis (MeOH): λ_{max} = 410 nm.– ^{1}H NMR (DMSO-d_6) δ = 14.83 (s*, 1H, NH), 11.74 (br.*, 1H, OH), 7.50 (s, 1H, Im-2-H), 8.72 (d, *J* = 5.0 Hz, 1H, Py-2-H, Py-6-H), 7.20 (m, 1H, Ph-5-H), 6.98 (m, 3H, Ph-6-H, Py-3-H, Py-5-H), 6.65 (s, 1H, Im-5-H), 6.33 (dd, $^3J_{H,F}$ = 9.7 Hz, $^4J_{H,H}$ = 3.1 Hz, 1H, Ph-3-H), 3.44 (m, 1H, CH), 2.72 (d, *J* = 6.3 Hz, 2H, CH_2), 1.17 (d, *J* = 6.3 Hz, 3H, CH_3).– MS (70 eV); *m/z* (%) = 324 (46) [M^+], 243 (100) [M^+– Im-CH_2]. Anal. ($C_{18}H_{17}FN_4O\cdot0.25H_2O$).

(R)-(–)-2-[[N-[1-(1H-Imidazol-4-yl)-2-propyl]imino](5-pyrimidinyl)-methyl]phenol (**8b**)

Crystallized from EtOAc/C_6H_{12} (63%), mp 81–83 °C, $[\alpha]^{20}_D$ = *–196.7* (c = 0.01 in MeOH).– UV/Vis (MeOH): λ_{max} = 404 nm.– ^{1}H NMR (DMSO-d_6) δ = 15.06 (br.*, 1H, NH), 11.74 (br.*, 1H, OH), 9.34 (s, 1H, Pym-2-H), 8.46 (s, 2H, Pym-4-H, Pym-6-H), 7.49 (s, 1H, Im-2-H), 7.31 (m, 1H, Ph-5-H), 6.93 (d, ^3J = 8.1 Hz, 1H, Ph-6-H), 6.70 (m, 2H, Im-2-H, Ph-4-H), 6.58 (dd, ^3J = 8.0 Hz, ^4J = 1.5 Hz, 1H, Ph-3-H), 3.36 (m, 1H, CH), 2.74 (d, *J* = 6 Hz, 2H, CH_2), 1.22 (d, 3H, *J* = 6.2 Hz, 3H, CH_3). MS (70 eV); *m/z* (%) = 307 (10) [M^+], 226 (100) [M^+–Im-CH_2]. Anal. ($C_{17}H_{17}N_5O\cdot C_2H_5OH$) C, H: calcd, 6.56; found, 6.09; N.

(R)-(–)-4-Fluoro-2-[[N-[1-(1H-imidazol-4-yl)-2-propyl]imino]-(1H-pyrrol-2-yl)methyl]phenol (**8c**)

Crystallized from EtOAc/C_6H_{12} (46%), mp 108–110 °C, $[\alpha]^{20}_D$ = *–148.5* (c = 0.01 in MeOH).– UV/Vis (MeOH): λ_{max} = 420 nm.– ^{1}H NMR ($CDCl_3$) δ = 7.51 (s, 1H, Im-2-H), 7.13 (dd, $^3J_{H,F}$ = 10.1 Hz, $^4J_{H,H}$ = 3.1 Hz, 1H, Ph-3-H), 7.06 (s, 1H, Pyr-H), 6.94 (m, 1H, Ph-5-H), 6.78 (m, 2H, Ph-6-H, Im-5-H), 6.35 (s, 2H, 2 Pyr-H), 4.59 (m, 1H, CH), 2.95 (m, 2H, CH_2), 1.26 (d, *J* = 6.2 Hz, 3H, CH_3).– MS (70 eV); *m/z* (%) = 312 (5) [M^+], 231 (24) [M^+ –Im-CH_2]. Anal. ($C_{17}H_{17}FN_4O\cdot0.25H_2O$).

(R)-(–)-4-Fluoro-2-[[N-[1-(1H-imidazol-4-yl)-2-propyl]imino]-(2-furanyl)methyl]phenol (**8d**)

Crystallized from EtOAc/C_6H_{12} (60%), mp 121 °C, $[\alpha]^{20}_D$ = *–177.8* (c = 0.01 in MeOH).– UV/Vis (MeOH): λ_{max} = 428 nm.– ^{1}H NMR ($CDCl_3$) δ = 7.56 (s, 1H, Fu-5-H), 7.49 (s, 1H, Im-2-H), 7.02 (m, 1H, Ph-5-H), 6.91 (dd, $^3J_{H,H}$ = 9.0 Hz, $^4J_{H,F}$ = 4.9 Hz, 1H, Ph-6-H), 6.75 (m, 1H, Im-5-H, Ph-3-H), 6.52 (d, 1H, Fu-H), 6.36 (d, *J* = 3.4 Hz, 1H, Fu-H), 3.97 (m, 1H, CH), 2.91 (d, *J* = 6.3 Hz, 2H, CH_2), 1.32 (d, *J* = 6.3 Hz, 3H, CH_3).– MS (70 eV); *m/z* (%) = 313 (35) [M^+], 232 (100) [M^+–Im-CH_2]. Anal. ($C_{17}H_{16}FN_3O_2$).

(R)-(–)-4-Fluoro-2-[[N-[1-(1H-imidazol-4-yl)-2-propyl]imino]-(3-furanyl)methyl]phenol (**8e**)

Crystallized from EtOAc/C_6H_{12} (72%), mp 138 °C, $[\alpha]^{20}_D$ = *–239.5* (c = 0.01 in MeOH).– UV/Vis (MeOH): λ_{max} = 412 nm.– ^{1}H NMR ($CDCl_3$) δ = 7.52 (m, 2H, Fu-H, Im-2-H), 7.16 (s, 1H, Fu-H), 6.98 (m, 1H, Ph-5-H), 6.88 (dd, ^3J = 9.0 Hz, ^4J = 4.8 Hz, 1H, Ph-6-H), 6.73 (m, 2H, Im-5-H, Ph-3-H), 6.14 (s, 1H, Fu-H), 3.92 (m, 1H, CH), 2.88 (d, *J* = 6.4 Hz, 2H, CH_2), 1.25 (d, *J* = 6.3 Hz, 3H, CH_3).– MS (70 eV); *m/z* (%) = 313 (14) [M^+], 232 (100) [M^+–Im-CH_2]. Anal. ($C_{17}H_{16}FN_3O_2$).

(R)-(–)-4-Fluoro-2-[[N-[1-(1H-imidazol-4-yl)-2-propyl]imino]-(2-thienyl)methyl]phenol (**8f**)

Crystallized from Et_2O (75%), mp 154–156 °C, $[\alpha]^{20}_D$ = *–202.0* (c = 0.01 in MeOH).– UV/Vis (MeOH): λ_{max} = 420 nm.– ^{1}H NMR (DMSO-d_6) δ = 14.85 (br.*, 1H, NH), 11.74 (br.*, 1H, OH), 7.85 (d, *J* = 4.9 Hz, 1H, Th-5-H), 7.49 (s, 1H, Im-2-H), 7.21 (m, 2H, Ph-5-H, Th-H), 7.00 (s, 1H, Th-H), 6.92 (dd, $^3J_{H,H}$ = 9.0 Hz, $^4J_{H,F}$ = 4.8 Hz, 1H, Ph-6-H), 6.66 (s, 1H, Im-5-H), 6.48 (dd, $^3J_{H,F}$ = 9.6 Hz, $^4J_{H,H}$ = 3.1 Hz, 1H, Ph-3-H), 3.73 (m, 1H, CH), 2.77 (d, 2H, CH_2), 1.20 (d, *J* = 6.2 Hz, 3H, CH_3).– MS (70 eV); *m/z* (%) = 329 (31) [M^+], 248 (100) [M^+–Im-CH_2]. Anal. ($C_{17}H_{16}FN_3OS$).

(R)-(–)-4-Fluoro-2-[[N-[1-(1H-imidazol-4-yl)-2-propyl]imino]-(3-thienyl)methyl]phenol (**8g**)

Crystallized from EtOAc/C_6H_{12} (79%), mp 142 °C, $[\alpha]^{20}_D$ = *–227.5* (c = 0.01 in MeOH).– UV/Vis (MeOH): λ_{max} = 414 nm.– ^{1}H NMR (DMSO-d_6) δ = 15.22 (s*, 1H, NH), 11.75 (br.*, 1H, OH), 7.78 (dd, ^3J = 4.9 Hz, ^4J = 2.9 Hz, 1H, Th-5-H), 7.49 (m, 2H, Im-2-H, Th-2-H), 7.17 (m, 1H, Ph-5-H), 6.92 (dd, $^3J_{H,H}$ = 9.0 Hz, $^4J_{H,F}$ = 4.8 Hz, 1H, Ph-6-H), 6.88 (d, *J* = 4.6 Hz, 1H, Th-4-H), 6.65 (s, 1H, Im-5-H), 6.38 (dd, $^3J_{H,F}$ = 9.9 Hz, $^4J_{H,H}$ = 3.1 Hz, 1H, Ph-3-H), 3.64 (m, 1H, CH), 2.74 (d, *J* = 6.4 Hz, 2H, CH_2), 1.16 (d, *J* = 6.3 Hz, 3H, CH_3).– MS (70 eV); *m/z* (%) = 329 (24) [M^+], 248 (100) [M^+ Im-CH_2]. Anal. ($C_{17}H_{16}FN_3OS$).

Single X-Ray Analysis of 8d. Precise lattice parameters and three dimensional intensity data were measured at room temperature on a Stoe-diffractometer using Ni-filtered CuKα radiation (λ = 1.5418 Å). The intensity data set was corrected for Lorentz and polarization effects but not for absorption. Phase determination was made with direct methods (program SHELXS86)[28]; refinement was done with the corresponding least-squares programs of the XTAL program system (version 3.2, 1992)[29]. All hydrogen atoms were located from difference syntheses. 273 Parameters were used in the final refinements; a $1/\sigma^2(F_o)$ weighting scheme was used; $\sigma(F_o)$ was from counting statistics. No significant peaks or holes were seen in a final difference Fourier map.

Crystal Data of 8d. Crystals of **8d**, molecular formula $C_{17}H_{16}FN_3O_2$ (M_r = 313.3), were grown from EtOAc/light petroleum (bp 50–70 °C). Space group, orthorhombic $P2_12_12_1$; unit cell, a = 18.263 (3) Å, b = 9.800 (1) Å, c = 9.049 (2) Å, V = 1619.6 (5) Å^3, Z = 4, ρ_x = 1.285 g cm^{-3}, μ (CuKα) = 7.96 cm^{-1}. A single crystal with dimensions 0.33 × 0.13 × 0.13 mm was used to collect the intensity data of 1568 independent reflections ($\theta \leq 64°$; h, k, l all ≥ 0) by using the ω–2θ scan technique. An intensity variation of less than 2.0%, monitored via three check reflections, was considered insignificant. A total of 368 reflections with $F_o \leq \sigma(F_o)$ were coded unobserved. After convergence, R values of R = 0.036 and R_w = 0.023 were obtained.

Pharmacology. Both the determination of the prodrug *in vitro* hydrolysis rates and the *in vivo* parameters of **1** and **8** were performed according to ref.[21].

Determination of the Prodrug Hydrolysis Rates *in Vitro*. An extemporaneously prepared 10 mM solution of **8** in DMSO was diluted to a final concentration of 4 µM in 0.4 N $HClO_4$ or in 0.05 M K_2HPO_4/KH_2PO_4 buffer pH 7.4 and incubated at room temperature. An aliquot was taken at various time intervals, diluted and brought up to a final concentration of 0.4 N $HClO_4$. Immediately after incubation **1** was measured by a sensitive and specific RIA developed according to a principle already described[30]. Briefly the perchloric samples or standards were derivatized with *p*-benzoquinone during a 30 min incubation at room temperature. These derivatized samples were then incubated with an antiserum raised in rabbits for one hour at 37 °C and left at 4 °C overnight after transfer in swine antirabbit IgGcoated 96-well plates and addition of an [^{125}I]iodinated tracer. The radioactivity bound to the wells was then counted in a gamma–spectrometer with an efficiency of 82%. The hydrolysis rate of **8** was calculated as the percent ratio of the level of **1** measured in the sample and that corresponding to a complete hydrolysis of the prodrug.

Determination of 1 and Prodrug Levels in Plasma and Cerebral Cortex of Mice Treated with the Various Prodrugs. Male Swiss mice (20–25 g, Iffa-Credo, France), that were given food and water *ad libitum*, received an oral dose of 24 µmol/kg of **8** in 1% methylcellulose and were then sacrificed by decapitation 0.5, 1, 3, or 6 h later. Controls received the vehicle only. For determination of **1** and prodrug (**8**) levels in plasma and cerebral cortex, blood was collected after decapitation, centrifuged (15000*g* for 1 min), and the supernatant was brought up to a final concentration of 0.4 N $HClO_4$.The cerebral cortex was dissected out rapidly and homogenized in 10 volumes (*w/v*) of ice-cold 0.4 N $HClO_4$. Plasma and cerebral extracts were then centrifuged and the clear supernatant was used for the RIA immediately or stored at –20 °C. Before use one aliquot of the $HClO_4$ extract was heated at 95 °C for 30 min to allow the total *in vitro* hydrolysis of the prodrug, while another one was used without heating. Compound **1** was derivatized and then radioimmunoassayed in the non-heated and heated extracts. The level of **8** was calculated as the difference between these two determinations. The plasma from non-treated mice was also assayed in order to estimate the interference of plasma in the RIA for **1**. The determinations of **1** for treated mice were then corrected accordingly.

References

☆ Dedicated to Prof. Dr. Dr. E. Mutschler, Frankfurt/Main, on the occasion of his 65th birthday.

[1] J.-M. Arrang, M. Garbarg, J.-C. Schwartz, *Nature (London)* **1983**, *302*, 832–837.

[2] J.-M. Arrang, M. Garbarg, J.-C. Schwartz, *Neuroscience* **1985**, *15*, 553–562.

[3] J.-M. Arrang, M. Garbarg, J.-C. Schwartz, *Neuroscience* **1987**, *23*, 149–157.

[4] J. Clapham, G.J. Kilpatrick, *Br. J. Pharmacol.* **1992**, *107*, 919–923.

[5] E. Schlicker, K. Fink, M. Detzner, M. Göthert, *J. Neural. Transm. [GenSect]* **1993**, *93*, 1–10.

[6] K. Fink, E. Schlicker, M. Göthert, *Adv. Biosci.* **1991**, *82*, 125–126.

[7] E. Schlicker, R. Betz, M. Göthert, *Naunyn-Schmiedebergs Arch. Pharmacol.* **1988**, *337*, 588–590.

[8] J.-M. Arrang, B. Devaux, J.-P. Chodkiewicz, J.-C. Schwartz, *J. Neurochem.* **1988**, *51*, 105–108.

[9] H. Pollard, J. Moreau, J.-M. Arrang, J.-C. Schwartz, *Neuroscience* **1993**, *52*, 169–189.

[10] X. Ligneau, M. Garbarg, M.L. Vizuette, J. Diaz, K. Purand, H. Stark, W. Schunack, J.-C. Schwartz, *J. Pharmacol. Exp. Ther.* **1994**, *271*, 452–459.

[11] G. Bertaccini, G. Corruzzi, in *The Histamine Receptor, Receptor Biochemistry and Methodology* (Eds.: J.-C. Schwartz, H. L. Haas), Wiley-Liss, Inc., New York, **1992**, chapter 10, pp 193–230.

[12] P.J. Barnes, in *The Histamine Receptor, Receptor Biochemistry and Methodology* (Eds.: J.-C. Schwartz, H.L. Haas), Wiley-Liss, Inc., New York, **1992**, chapter 12, pp 253–270.

[13] G. Gerhard, W. Schunack, *Arch. Pharm. (Weinheim)* **1980**, *313*, 709–714.

[14] J.-M. Arrang, M. Garbarg, J.-C. Lancelot, J.-M. Lecomte, H. Pollard, M. Robba, W. Schunack, J.-C. Schwartz, *Nature (London)* **1987**, *327*, 117–123.

[15] R. Lipp, J.-M. Arrang, M. Garbarg, P. Luger, J.-C. Schwartz, W. Schunack, *J. Med. Chem.* **1992**, *35*, 4434–4441.

[16] S. Yamazaki, E. Sakurai, N. Hikichi, N. Sakai, K. Maeyama, T. Watanabe, *J. Pharm. Pharmacol.* **1994**, *46*, 371–374.

[17] L.B. Hough, J.K. Khandelwal, T.W. Mittag, *Agents Actions* **1981**, *11*, 425–428.

[18] A. Rouleau, M. Garbarg, X. Ligneau, C. Mantion, P. Lavie, C. Advenier, J.-M. Lecomte, M. Krause, H. Stark, W. Schunack, J.-C. Schwartz, *J. Pharmacol. Exp. Ther.*, submitted.

[19] M. Garbarg, J.-M. Arrang, W. Schunack, R. Lipp, H. Stark, J.-M. Lecomte, J.-C. Schwartz, PCT Int. Appl. WO 91/17 146. **1991** [Chem. Abstr. **1992**, *116*, P194311]

[20] W. Schunack, H. Stark, *Eur. J. Drug Metab. Pharmacokinet.* **1994**, *3*, 173–178.

[21] M. Krause, A. Rouleau, H. Stark, P. Luger, R. Lipp, M. Garbarg, J.-C. Schwartz, W. Schunack, *J. Med. Chem.* **1995**, *38*, 4070–4079.

[22] J.-P. Kaplan, B.M. Raizon, M. Desarmien, P. Feltz, P.M. Headly, P. Worms, K.G. Lloyd, G. Bartholini, *J. Med. Chem.* **1980**, *23*, 702–704.

[23] J. Jílek, J. Pomykácek, H. Frycová, Z. Polívka, *Cesk. Farm.* **1990**, *39*, 249–253.

[24] J.-M. Lecomte, et al. Unpublished Results.

[25] A. Einhorn, F. Hollandt, *Ann. Chem.* **1898**, *301*, 95–101.

[26] K. Fries, G. Finck, *Ber. Dtsch. Chem. Ges.* **1908**, *41*, 4271.

[27] E. Keller, *SCHAKAL86, Program for the Graphic Representation of Molecular and Crystallographic Models*; University of Freiburg: Germany, 1986.

[28] G.M. Sheldrick, In *Crystallographic Computing 3* (Eds.: G. M. Sheldrick, C. Krüger, R. Goddard), Oxford University Press, Oxford, **1985**, pp 175–198.

[29] J.M. Stewart, H.D. Flack, S.R. Hall, Eds. *XTAL Program System 3.2, Users Manual*; University of Western Australia, Geneva and Maryland, 1992.

[30] M. Garbarg, H. Pollard, M. D. Trung Tuong, J.-C. Schwartz, C. Gros, *J. Neurochem.* **1989**, *53*, 1724–1730.

[31] J.W. Black, C.R. Ganellin, *Experientia* **1974**, *30, 111–113.*

Received: January 22, 1996 [FP088]